Progress In Electromagnetics Research M, Vol. 72, 165–174, 2018

Fabrication and Pressure Sensing Characterization of an Ultrathin Egg-Shaped Microbubble

Guanjun Wang[1, 2], Mengxing Huang[1, 2, *], Jinrong Liu[3], Yuhang Li[1, 2], Shubin Zhang[1, 2], Xuefen Wan[4], Muhammad S. Sardar[5], Jianning Han[3], Qingche Song[3], and Zhiguo Gui[3],

Abstract—In this paper, an ultrathin egg-shaped microbubble was proposed and analyzed for pressure sensing firstly, which was fabricated by utilizing an improved pressure-assisted arc discharge technique. By tailoring the arc parameters and the position of glass tube during the fabrication process, the thinnest wall of the fabricated microbubble could reach 873 nm. Such an ultrathin film structure is very suitable for pressure sensing. Especially, as only a commercial fusion splitter and pressure pump were utilized to achieve such functions, the fabrication cost was very cheap. The fiber Fabry-Perot (FP) interference technique was used to analyze its pressure sensitivity by filling the inner wall of the microbubble with different air pressures. The experiment results depicted that the end face of microbubble expands with the increase of the filling pressure. The pressure sensitivity of such an egg-shaped microbubble could reach up to 14.3 pm/kPa in terms of interference spectrum shift, while the maximum cavity deformation sensitivity of the microbubble vs. pressure could reach up to 0.334 nm/kPa in terms of cavity length change. Besides, the maximum sensitivity vs. temperature was only 27.83 pm/°C. Results of this study could be good reference for developing new pressure sensors with low cost, high sensitivity and good anti-temperature interference abilities.

1. INTRODUCTION

Pressure measurement has many important applications, such as urban pipeline water supply and oil production [1, 2], while the fiber optical sensors, especially the fiber Fabry-Perot (FP) sensor, should be good candidates for high sensitive pressure measurement. The fiber FP pressure sensors with a structure of thin film end face have many advantages, such as high sensitivity, low fabrication and maintenance cost, long detection distance, easy to connect and others. As the thickness of end film was closely related with the pressure sensitivity, reducing the film thickness and expanding the film surface could be good ways for enhancement of pressure sensitivity.

Currently, many methods have been proposed for immobilizing a fiber probe with thin film, such as MEMS technology [1], graphene or other membrane [3], silk fibroin diaphragm [4], Focused Ion Beam (FIB) Milling [5], chemical etching [6], end polishing [7], and arc discharge [8]. For example, Wu et al. developed a new silicon process to construct a monolithic photonic crystal-based crystalline silicon membrane. An order of magnitude more sensitive, with a spectral shift sensitivity magnitude up to 8.6 nm/kPa was attained [1]. Such kind of pressure sensor could also be utilized for acoustic sensing [2]. As the MEMS technology has good control ability in terms of film thickness and surface area, the

Received 6 May 2018, Accepted 18 July 2018, Scheduled 29 August 2018

* Corresponding author: Mengxing Huang (huangmx09@hainu.edu.cn).

[1] State Key Laboratory of Marine Resource Utilization in South China Sea, Hainan University, Haikou 570228, China. [2] Collage of Information Science & Technology, Hainan University, Haikou 570228, China. [3] School of Information and Communication Engineering, North University of China, Taiyuan 030051, China. [4] Department of Computer Science and Technology, North China Institute of Science and Technology, Sanhe 065201, China. [5] College of Information Science and Technology, Donghua University, Shanghai 201620, China.

sensitivity of MEMS-based fiber pressure sensor was generally high, and its uniformity was generally good, but the drawback was its expensive cost. Due to higher mechanical strength and ultrathin thickness, graphene was also used as a sensitive diaphragm in a Fabry-Perot cavity to improve the sensitivity of pressure sensors [3]. An extremely thin 13-layered 125 μm diameter graphene diaphragm is fabricated on the tip of the fiber end. Other inexpensive methods were also proposed for pressure sensitivity enhancement. Kou et al. proposed to build a miniature fiber-optic Fabry-Perot on the tip of a single mode fiber with a thin silk fibroin film [5]. The result shows good air tightness with a response of 12.3 nm/kPa in terms of cavity length change. However, the sensitivity of such simple fabrication methods was relatively low. Focused ion beam (FIB) milling was a better technology for fiber pressure sensing due to its tiny and convenient spot size (on the order of a few tens of nm), while the fabrication was very expensive [5]. A Fabry-Perot cavity and a thin silica diaphragm could also be fabricated by wet chemical etching and fusion splicing [6]. However, the film roughness etched by HF solution was relatively large, which impacts the output spectral of Fabry-Perot interference greatly. Besides, the film thickness control ability of end polishing method was usually poor, and the success rate was relatively low [7].

The fiber film fabricated by arc discharge method could reach the level of micrometer in the previous report [8]. However, it seems that the thinner area of bubble tip was very small, which restricts its sensitivity much more. The pressure-assisted arc discharge methods were also used for producing microbubble in previous reports [9–11]. It seems that the shortcomings of this structure, especially the poor symmetry and uniformity of single-ended microbubbles, have affected its potential for low-density moire mode sensing and Fabry-Perot pressure sensing.

For decreasing the film thickness and expanding the film area simultaneously, the pressure-assisted arc discharge technique was improved in this paper to fabricate an egg-shaped microbubble. Such a microbubble was also further directly utilized for high sensitive pressure measurement. Compared with previous reports, a low-current and slow-release discharge strategy was adopted here to inflate such a microbubble. By controlling the arc discharge intensity, time, and fiber position strictly, this technique could improve the symmetry of the microbubble effectively and reduce the thickness of the end film to the scale of 873 nm. Moreover, only a commercial fusion splitter and pressure pump splitter were used, which has special attraction for mass production. Such a structure was also utilized for highly sensitive pressure measurement. And the maximum cavity deformation sensitivity vs. pressure could reach up to 0.334 nm/kPa in terms of cavity length change. A 0.7 kPa pressure sensitivity resolution was confirmed in our experiment, and the maximum sensitivity vs. temperature was only 27.83 pm/°C.

2. FABRICATION OF THE EGG-SHAPED MICROBUBBLE

The schematic diagram of fabrication process of the proposed egg-shaped microbubble was depicted in Fig. 1. A commercial fusion splitter (Fujikura 60S), pressure pump, single mode fiber and glass tube were used here. AS depicted in the schematic diagram, a silica glass tube with inner/outer diameter of 75 μm/125 μm was fused with a common single-mode silica fiber firstly. Then an atmosphere pressure about 120 kPa (absolute pressure value, the same below) was filled into the glass tube from the other end by a pressure pump. Here the specific filling pressure value depends on the thickness of glass tube, the following outward force and arc discharge intensity. Pressure of the pressure pump, whether too large or too small, will influence the possibility of success of microbubble fabrication. Then the glass tube was moved towards the electrode region. An outward force from the motors was imposed on the glass tube by moving the motors towards to the outer directions. Then we align the electrodes of the fusion splicer with the glass tube and press the button to discharge several times under the condition of filling the glass with air pressures. Correspondingly, two hollow cone structures were shaped at the disrupt place. Thirdly, one pressure-filled cone connected with the glass tube was placed vertically near the two electrodes. Then discharges several times once more. A microbubble with a spherical structure but thick wall was shaped afterwards. The parameters of arc intensity and discharge time utilized here were −5 BIT and 300 ms. Here the BIT is the unit of discharge power of fusion splitter (Fujikura 60S). The utilized air pressure value was near 120 kPa. Finally, the end face of pressure-filled microbubble was moved near the center of electrodes and discharged again. In this way, the expansion effect of the end face was more obvious, which makes it very thin after the discharge. As the final shape of microbubble

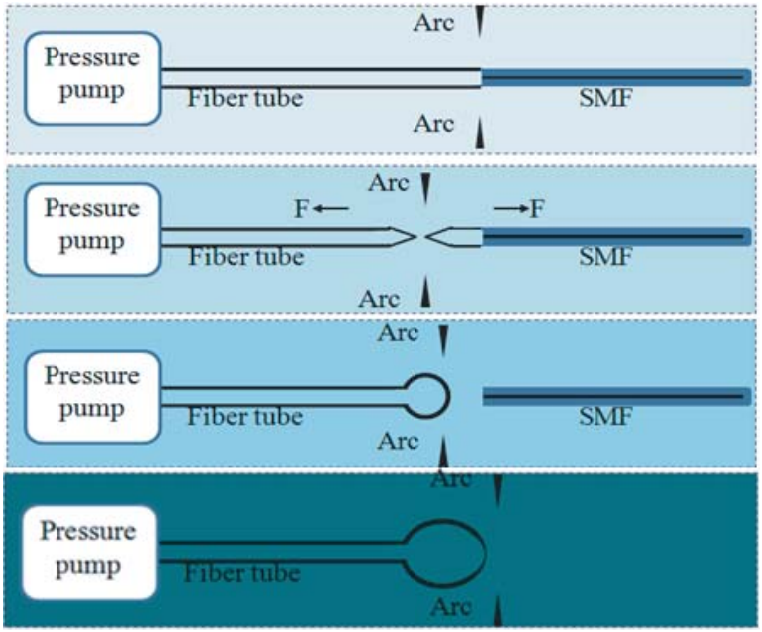

Figure 1. Schematic diagram of Fabrication process.

was like an egg, we named it egg-shaped microbubble. By controlling the discharge parameters, the thickness of the end face could be very thin without burst. Besides, the thin surface region was relatively larger than that in previous reports, which makes it suitable for high sensitivity pressure measurement.

Figure 2 shows the experimental setup of a pressure filling system. Since one end of the glass tube is connected to the pressure pump, air is generated via the pressure pump and transmitted through the glass tube into the microbubbles. The specific pressure value could be read from the pressure gauge of the right side. In the following experiment of pressure sensitivity measurement, the pressure filling system was similar.

Figures 3(a) and 3(b) show photographs of the fabricated microbubbles under the steps of three and four. From Fig. 2(a), we can see that the fabricated microbubble after the third step has a spherical surface, thick and uniform wall (from the vertical view, X axis). As depicted in Fig. 2(b), the final microbubble has a thin end face due to the expansion effect during the last step. It was revealed from

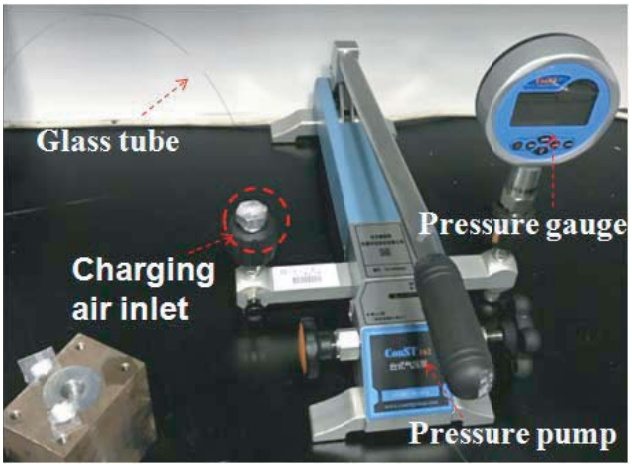

Figure 2. Experimental setup of pressure filling system.

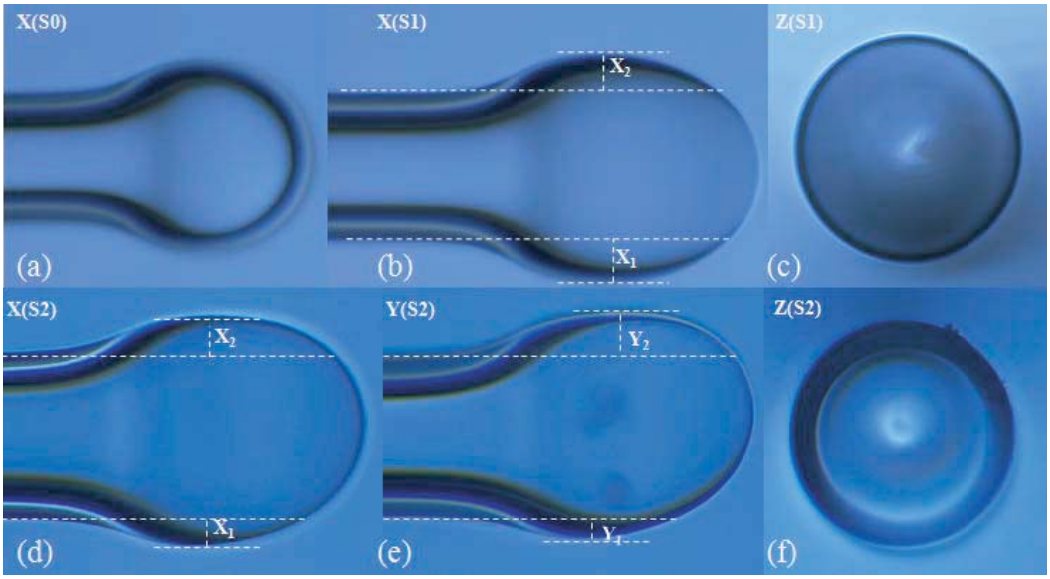

Figure 3. Microscopy photographs of the fabricated microbubbles under the step of three (S0) and four (S1 and S2).

Fig. 2(c) that the symmetry of microbubble was also improved in this improved pressure-assisted arc discharge technique.

For analyzing the symmetry of microbubble quantificationally, parameters X_1, X_2, Y_1 and Y_2 were used here to denote the specific inflation degree of different sides from the vertical and lateral views. Thus, the ratios $\gamma_X = X_1/X_2$ and $\gamma_Y = Y_1/Y_2$ mean the unevenness of inflation of X axis and Y axis. Two egg-shaped microbubbles were fabricated in this paper. For sample 1 (S1) (Fig. 3(b) and Fig. 3(c)), the values of X_1 and X_2 were 33 μm and 37 μm, so γ_X of S1 was 89%. For sample 2 (S2) (Fig. 3(d), Fig. 3(e) and Fig. 3(f)), the values of X_1, X_2, Y_1 and Y_2 were 42.3 μm, 53.4 μm, 32.3 μm and 64.7 μm, respectively, so γ_X and γ_Y of S_2 were 79% and 50%. So, we recognized that this improved pressure-assisted arc discharge method could decrease the thickness and improve the symmetry at the best. However, the unevenness still existed due to the influence of gravity.

For measuring the wall thickness of the microbubble accurately, a scanning electron microscope (SEM) was used to measure the accurate wall thickness afterwards. Before the SEM experiment, the fabricated microbubble was punctured with a tapered fiber. It was depicted from Fig. 4 that

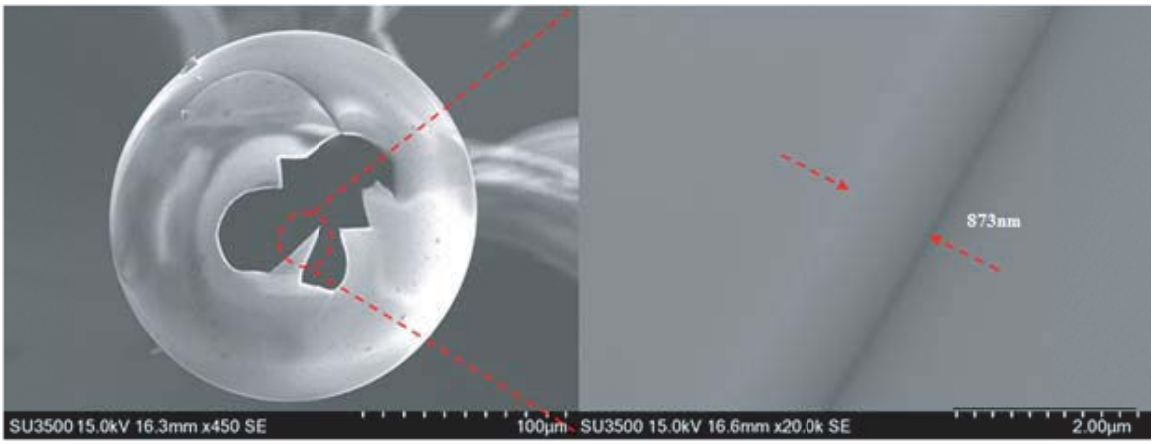

Figure 4. SEM photograph of the fabricated egg-shaped microbubble.

the thickness of microbubble could reach 873 µm at the center of the end face. It demonstrates that the proposed pressure-assisted arc discharge technique has significant potential in reducing the wall thickness. Especially, the thin region of end face was also large, which was of vast importance in the enhancement of pressure sensitivity, because the pressure sensitivity was proportional to the surface area and inversely proportional to the wall thickness.

3. SENSITIVITY CHARACTERIZATION OF THE EGG-SHAPED MICROBUBBLE

Subsequently, for measuring the pressure sensitivity of the fabricated microbubble, a Fabry-Perot interference experiment was carried out through the following setup, shown in Fig. 5. An FP interference sensing interrogator, a single mode fiber and a 3-dimensional platform were used. An FP interference spectrum was formed between the end of single mode fiber and the outer end of the microbubble. Such a spectrum was received by the interrogator afterwards. So a new fiber pressure sensor was shaped with key components of a microbubble, a single mode fiber and a 3-dimensional platform. The pitch d between the microbubble and the single-mode fiber could be calculated from the FP interference spectrum. The variety of FP interference spectrum under different filling pressures reflects the deformation Δd of the end face and the pressure sensitivity of the microbubble.

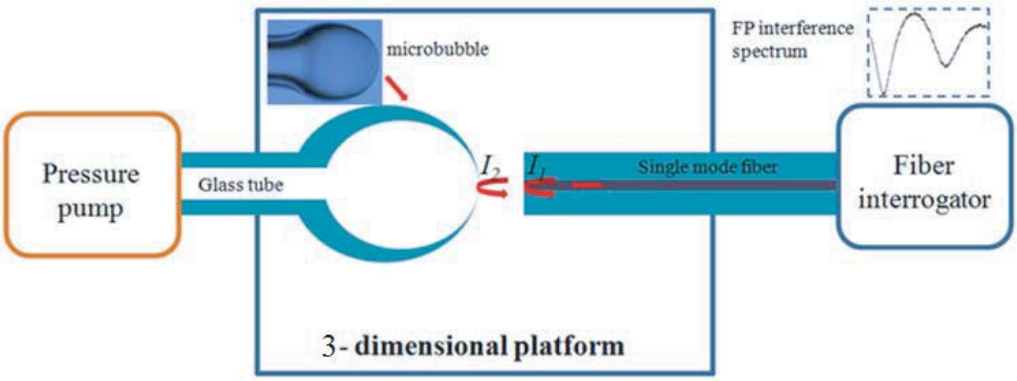

Figure 5. Schematic diagram of the pressure sensitivity measurement system.

The experimental setup of the 3-dimensional platform was shown in Fig. 6. Here the 3-dimensional platform was used to focus the single mode fiber and microbubble. This alignment procedure was monitored under the view of an industrial microscope.

The output light intensity of the FP interference spectrum could be expressed as:

$$I = I_1 + I_2 + 2\sqrt{I_1 I_2}\cos\gamma \tag{1}$$

where I_1 and I_2 were the light intensity of the two reflected waves, and γ was the difference of phase between the two reflected lights. Fig. 7(a) shows the shift of the FP interference spectrum between the single mode fiber and the outer end face of microbubble (S1) under different filling pressures (from 4 kPa to 1400 kPa). It seems that with the increase of filling pressure, the interference spectrum demonstrates a characteristic of blue shift. When the filling pressure was 4 kPa, the peak wavelengths of the interference peaks were around 1540 nm and 1585 nm. On the other hand, when the filling pressure was at 1400 kPa, the interference peaks were near 1525 nm and 1570 nm. The relationship of interference spectrum peaks/troughs and the filling pressure is depicted in Fig. 7(b). It seems that the spectral peak shift sensitivity vs. the filling pressure was about 14.3 pm/kPa.

Such sensitivity was similar to that in the previous reports [7] and was 15 times higher than that of [3]. However, the merit of this report is the low fabrication cost and simplified process.

For sample 2 (S2), when the filling pressure was increased from 4 kPa to 2400 kPa, a blue shift also appeared in the FP interference spectrum. After fine-tuning, the depth of contrast ratio of spectrum could reach 21 dB (Fig. 8(a)), which could be helpful for practical application. The corresponding

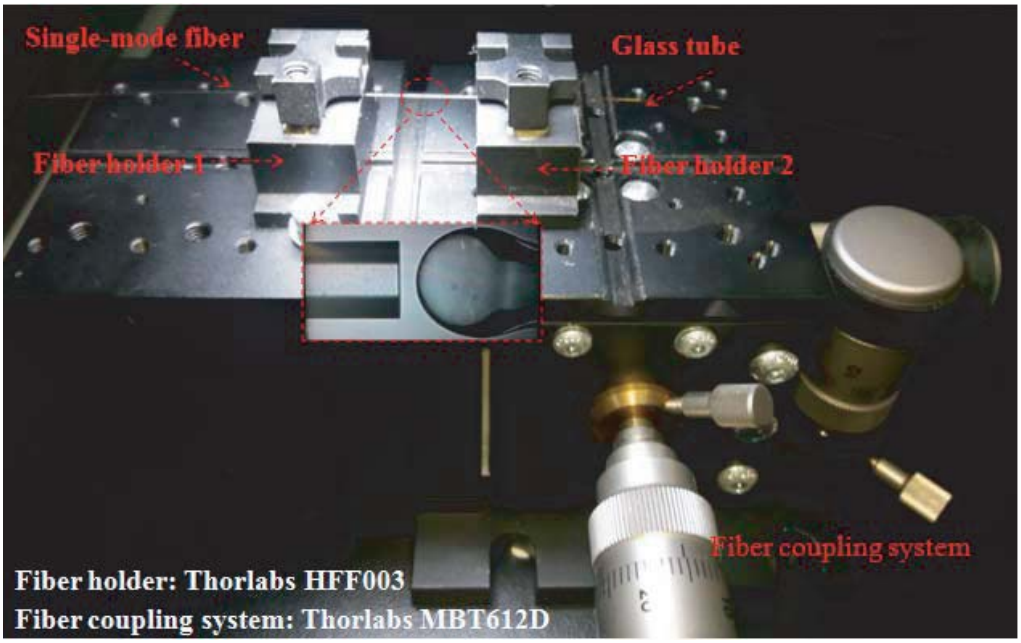

Figure 6. Experimental setup of the 3-dimensional platform.

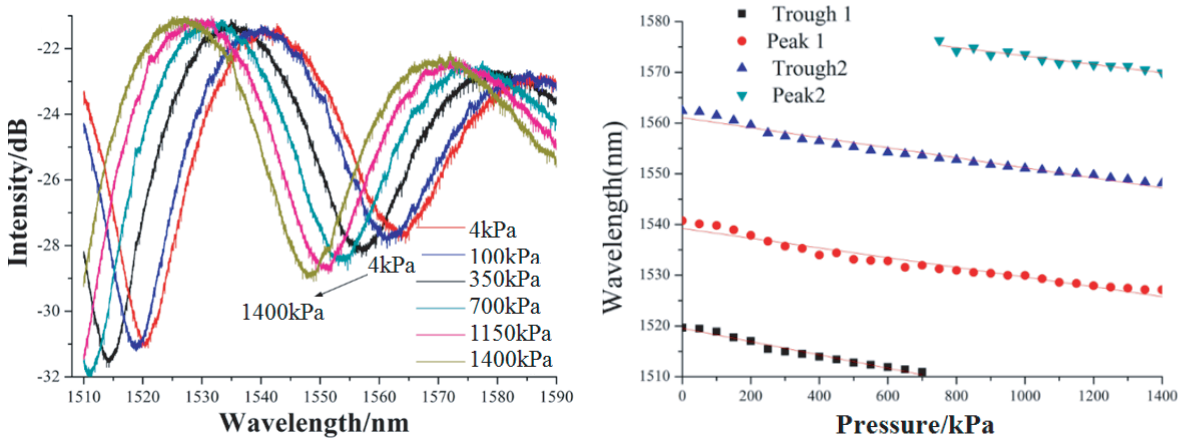

Figure 7. Result of Pressure sensitivity measurement experiment (S1). (a) FP interference spectrum between the singlemode fiber and the endface of microbubble under different filling pressures. (b) Relationship of interference spectrum shift and the filling pressure.

wavelength shift was also calculated in Fig. 8(b). It means that the pressure sensitivity of microbubble (S2) was about 11.1 pm/kPa, which is little lower than that of sample 1 (S1).

Besides, according to the theory of White-Light Interferometry [12], the corresponding pitch d between the fiber end and the end face of microbubble could be calculated from the FP interference spectrum.

$$d = \lambda_1\lambda_2\Delta\varphi/(4\pi(\lambda_1 - \lambda_2)) \tag{2}$$

Here, λ_1 and λ_2 mean the peak wavelength of FP interference spectrum, and $\Delta\varphi(\lambda)$ means the phase change. Especially mention that this work was done under the help of our cooperator Prof. Yi Jiang (Beijing Institute of Technology). Such a relationship was also demonstrated in Fig. 9. The corresponding relation of pitch d (μm) and pressure P (kPa) could be written as

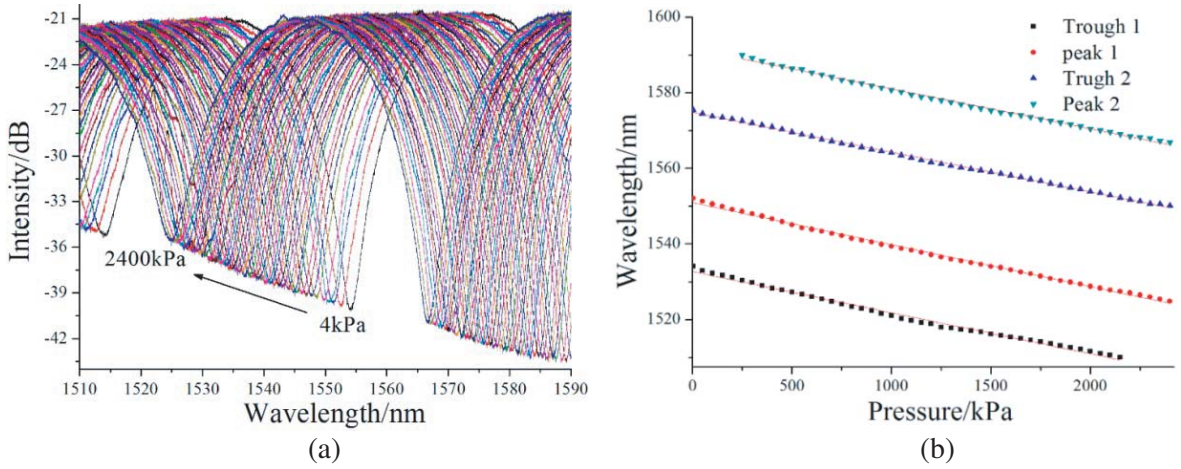

Figure 8. Result of Pressure sensitivity measurement experiment (S2). (a) Spectrum vs. pressure. (b) Wavelength shift vs. pressure.

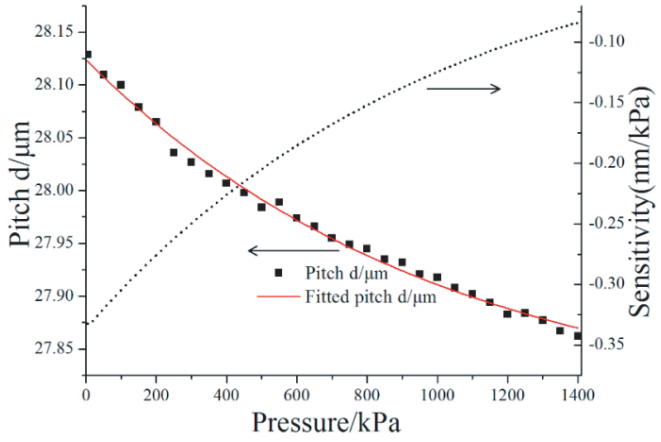

Figure 9. Relationship of microbubble deformation and filling pressure.

$d = 0.3393 * \exp(-P/1014.5) + 27.784$. Thus, the maximum cavity deformation sensitivity of the microbubble vs. pressure could reach up to 0.334 nm/kPa in terms of cavity length change. As the deformation resolution of the utilized interrogator could be up to 0.5 nm, a maximum pressure measurement resolution of 0.7 kPa could be attainable in our experiment.

For practical application, the proposed pressure sensor should be very integrated. So we tried to package the microbubble and single mode fiber on a glass substrate, and the material object is shown in Fig. 10(a). Fig. 10(b) is the microscopy view of packaged pressure sensor. Fig. 10(c) depicts the lateral view of package (schematic diagram). The fiber and microbubble was packaged by glue.

12 hours later after the packaging, the pressure sensitivity was measured again. It can be seen from Fig. 11(a) that the depth of contrast ratio of spectrum was decreased to 13 dB. With changing the filling pressure from 4 kPa to 2400 kPa, a blue shift of interference spectrum appeared, and the corresponding pressure sensitivity of microbubble (S2) after package was about 8.6 pm/kPa (Fig. 11(b)), which is little lower than before the packaging.

We think such a difference can be attributed to the distortion of package as the utilized glue could change the position relation of the end of microbubble and single mode fiber. The thickness of microbubble was not identical in every place, and the sensitivity to pressure was not the same. As the thickness of central end surface of microbubble was smaller than other places, its sensitivity should be the highest.

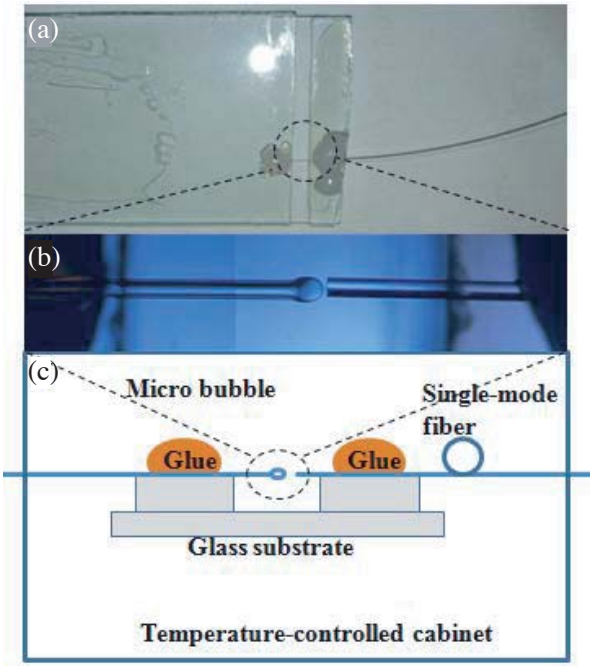

Figure 10. Package of the proposed pressure sensor.

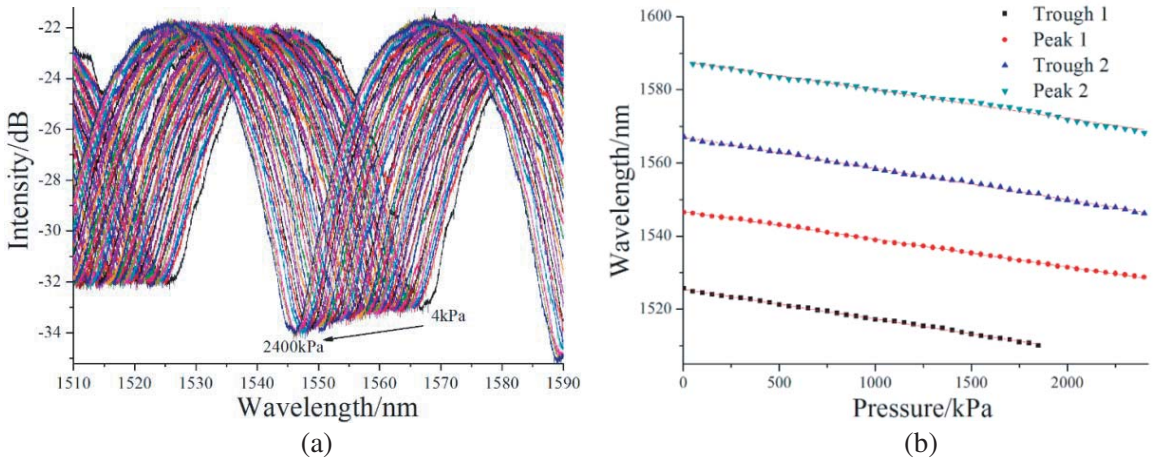

Figure 11. Result of Pressure sensitivity measurement experiment (S2) after package. (a) Spectrum vs. pressure after package. (b) Wavelength shift vs. pressure after package.

Besides, the temperature sensitivity of the package pressure sensor was also measured by placing the upper setup in a temperature-controlled cabinet. The corresponding results FP interference experiment from 25°C to 200°C are shown in Fig. 12. It was depicted that the corresponding wavelength shift of different peaks was only 4.34 nm/5.075 nm/4.81 nm when the chamber temperature rose from 25°C to 200°C. The corresponding maximum sensitivity vs. temperature was only 27.83 pm/°. Thus, we can believe that such a microbubble structure has good anti-temperature interference ability for high sensitivity pressure measurement. Such a temperature sensitivity is also consisted with the result of [5].

Finally, compared with other fiber pressure sensors of thin film structures, the proposed microbubble configuration has the following two merits. Firstly, the end face was very thin and the other parts relatively thicker. Thus, the end face place could contribute to sensitivity enhancement, and the other place could play the role of arm. Secondly, the measured pressure was filled into the inside but not

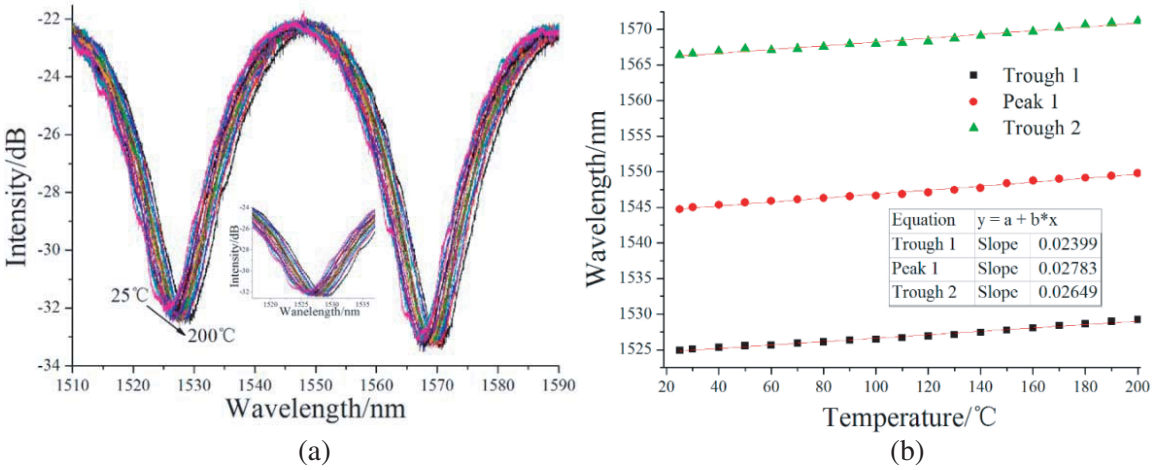

Figure 12. Result of FP interference experiment at different temperature (S2). (a) Spectrum vs. temperature. (b) Wavelength shift vs. temperature.

outside of the microbubble. When filling the microbubble with high pressure, the silica membrane molecular tension played a significant role in expansion, which was easy to suffer a large deformation. On the contrary, many microbubbles in previous reports can only measure the outside pressure. Due to the external extrusion effect, it was not easy to attain a large bubble deformation, which restricts their sensitivity potential. Finally, as the glass tube could play the role of guiding air pressure from one end to the other end, such a configuration could be used for remote pressure sensing.

4. CONCLUSIONS

In conclusion, an improved arc discharge method was proposed and analyzed for fabricating an ultra-thin egg-shaped microbubble, which was characterized by reducing the wall thickness of the microbubble end face on controlling the arc discharge intensity, time, and fiber position strictly, and using a rotating discharge method to improve the bubble symmetry. Besides, a low-current and slow-release discharge strategy was adopted here to inflate the bubble. It was proved that this method could effectively improve the symmetry of the microbubble and reduce the thickness of the end film to the scale of 873 nm. Compared with the conventional fiber-optic pressure sensors of thin-film structure, the fabricated microbubble has two advantages. On the one hand, the thickness of the microbubble end face was very thin, and its surface area is large. On the other hand, the measured pressure was sensed from the inside but not the outside of microbubble, which makes it easy to suffer a large deformation due to the membrane molecular tension effect. Our experiment result shows that a maximum cavity deformation sensitivity vs. pressure could reach up to 0.334 nm/kPa in terms of cavity length change. After package, the corresponding pressure sensitivity of microbubble (S2) was about 8.6 pm/kPa, and its temperature was only 27.83 pm/°C.

ACKNOWLEDGMENT

We thank the help of calculation of cavity length from our cooperator Prof. Yi Jiang (Beijing institute of technology).

Foundation items: National Natural Science Foundation of China (Grant #61865005, #61462022, Grant #61405127), National Key R&D Program (2016YFC0101603), National Key Technology Support Program (Grant #2015BAH55F04, Grant #2015BAH55F01), Major Science and Technology Project of Hainan province (Grant #ZDKJ2016015), Shaanxi Province Science Foundation for Youths (2018JQ6076).

REFERENCES

1. Wu, J. X., C. Jan, and O. Solgaard, "Single-crystal silicon photonic-crystal fiber-tip pressure sensors," *Journal of Microelectromechanical Systems*, Vol. 24, No. 4, 968–975, 2015.
2. Jan, C., W. Jo, M. J. F. Digonnet, and O. Solgaard, "Photonic-crystal-based fiber hydrophone with sub-100μPa/$\sqrt{}$Hz pressure resolution," *IEEE Photonics Technology Letters*, Vol. 28, No. 2, 123, 2016.
3. Li, C., J. Xiao, T. Guo, S. Fan, and W. Jin, "Interference characteristics in a Fabry-Perot cavity with graphene membrane for optical fiber pressure sensors," *Microsystem Technologies*, Vol. 21, No. 11, 2297–2306, 2015.
4. Cheng, L., C. Wang, Y. Huang, H. Liang, and B. O. Guan, "Silk fibroin diaphragm-based fiber-tip Fabry-Perot pressure sensor," *Optics Express*, Vol. 24, No. 17, 19600–19606, 2016.
5. Kou, J.-L., J. Feng, L. Ye, F. Xu, and Y.-Q. Lu, "Miniaturized fiber taper reflective interferometer for high temperature measurement," *Opt. Express*, Vol. 18, No. 13, 14245–14250, 2010.
6. Ge, Y., J. Zhou, and T. Wang, "A miniature extrinsic fiber Fabry-Perot pressure sensor based on fiber etching," *Proc. SPIE 8199, 2011 International Conference on Optical Instruments and Technology: Optical Sensors and Applications*, 81991L, November 22, 2011.
7. Wang, W., N. Wu, Y. Tian, X. Wang, C. Niezrecki, and J. Chen, "Optical pressure/acoustic sensor with precise Fabry-Perot cavity length control using angle polished fiber," *Opt. Express*, Vol. 17, No. 19, 16613–16618, 2009.
8. Liao, C., S. Liu, L. Xu, C. Wang, Y. Wang, Z. Li, Q. Wang, and D. N. Wang, "Sub-micron silica diaphragm based fiber-tip Fabry-Perot interferometer for pressure measurement," *Optics Letters*, Vol. 39, No. 10, 2827–2830, 2014.
9. Watkins, A., J. Ward, and Y. Wu, and S. N. Chormaic, "Single-input spherical microbubble resonator," *Optics Letters*, Vol. 36, No. 11, 2113–2115, 2011.
10. Yang, Y., S. Saurabh, J. M. Ward, and S. le Nic Chormaic, "High-Q, ultrathin-walled microbubble resonator for aerostatic pressure sensing," *Optics Express*, Vol. 24, No. 1, 294–299, 2016.
11. Henze, R., T. Seifert, J. Ward, and O. Benson, "Tuning whispering gallery modes using internal aerostatic pressure," *Optics Letters*, Vol. 36, No. 23, 4536–4538, 2011.
12. Jiang, Y., "Fourier transform white-light interferometry for the measurement of fiber optic extrinsic Fabry-Perot interferometric sensors," *IEEE Photon. Tech. Lett.*, Vol. 30, No. 2, 75–77, 2008.